Desalination and Water Treatment
www.deswater.com

17 (2010) 106–112
May

1944-3994/1944-3986
doi: 10.5004/dwt.2010.1705

Prediction of pervaporation performance of aqueous ethanol solutions based on single gas permeation

Jinhui Wang, Tomohisa Yoshioka, Masakoto Kanezashi, Toshinori Tsuru*

Department of Chemical Engineering, Graduate School of Engineering, Hiroshima University, 1-4-1 Kagayami-yama, Higashi-Hiroshima 739-8527, Japan
Tel: + (081) 082-424-7714; Email: tsuru@hiroshima-u.ac.jp

Received 31 July 2009; accepted 20 November 2009

ABSTRACT

In this study, pervaporation (PV) performance of porous silica membranes during dehydration of ethanol aqueous solutions was correlated with single gas permeation data in an attempt to predict PV performance. Porous silica membranes were prepared using a sol–gel technique with silica or cobalt-doped silica sols fired at different temperatures (from 350°C to 550°C) in air. Single gas permeation experiments were performed using pure gases (He, N_2, CO_2 and SF_6) at 200°C just after membrane preparation. PV experiments were carried out at 70°C at an ethanol feed concentration of 94 wt%. The time-course of PV performance and temperature-dependence for a single gas were investigated. The reproducibility of PV separation and gas permeation was investigated and confirmed. An attempt was made to find correlations between single gas permeation experimental data and PV separation performance. The permeance of He was reasonably well correlated with PV water flux. The permeance ratio of He/SF_6 was correlated with the PV separation factor.

Keywords: Pervaporation; Cobalt-doped silica membrane; ethanol dehydration; gas permeation

1. Introduction

Pervaporation (PV) is one of the most promising processes for separation of organic/water mixtures with very similar boiling or azeotropic points, such as ethanol water mixtures, as it offers significant energy and cost savings. Extensive research has been carried out to identify optimal membrane materials with high separation factor, flux and good stability [1]. Polymeric membranes are limited by their thermal and chemical instability, while porous inorganic membranes exhibit high permeability relative to dense membranes and high thermal stability relative to organic membranes. Because PV is widely used for dehydration of ethanol, development of a quick and effective method to predict separation performance is expected.

For prediction of PV separation performance, a mathematic model is used in most cases. The separation of feed components is based mostly on the selectivity of the membrane used. In turn, membrane selectivity is based on the differences in solubility and diffusivity of the membrane components. One of the simplest models for polymeric membranes is the solution–diffusion mechanism where permeating molecules dissolve and diffuse through a membrane. Lovasz et al. proposed the use of a modified Rautenbach model to simulate PV performance [2]. Water–ethanol as a binary mixture and water-ethanol-2-propanol as a ternary one, were separated using a PERVAP 2210 PVA/PAN composite membrane. Good agreement was obtained between measured and simulated data. Ma et al. [3]

*Corresponding author

Presented at the Fifth Conference of the Aseanian Membrane Society Aseania 2009 "Recent Progress in Membrane Science and Technology", 12–14 July 2009, Kobe, Japan.

analyzed PV dehydration performance of ethanol aqueous solutions using the adsorption–diffusion model, which was originally proposed by van Leeuwen [4] for porous ceramic membranes, and discussed the effects of temperature and concentration on PV performance.

Yang and coworkers proposed a permeation model in which a conical pore structure was assumed, with the small radius (neck) at the top of the separation membrane [5]. PV of aqueous solutions of acetone, IPA or dioxane was performed using a microporous SiO_2–ZrO_2 membrane. Water permeation through the micropores was found to be not simply proportional to the partial water vapor pressure of the feed, but, rather, showed a complicated dependence on capillary suction pressure, osmotic pressure and on partial water vapor pressure. The validity of the model was established, and the model was capable of predicting water flux during PV of aqueous mixtures of various organic solvents. However, information regarding prediction of the separation factor is yet to be reported.

For prediction of gas separation, Thornton et al. [6] employed a mathematical model, using the Lennard-Jones interactions between gas molecules and the pore wall, to determine the mechanisms of gas diffusion that occur within pores of different sizes, shapes and compositions. Different critical pore sizes were used to indicate the division of the three diffusion regimes, namely, activation diffusion, surface diffusion and Knudsen diffusion. Using this model, one can predict the separation outcome of a variety of membranes for which pore shape, size and composition are known; conversely, pore characteristics can be predicted from known permeation rates.

As mentioned above, for prediction of PV or gas separation performance, a transport model that includes many membrane-related parameters (membrane thickness, pore shape, pore size or distribution, etc.) as well as characteristics of the permeating molecules (molecular size, shape, etc.) is required. However, such a complicated model is quite difficult for practical applications. In the present study, we propose a method to predict PV performance that is based only on single gas permeation data. Porous silica membranes were prepared using silica and cobalt-doped silica sols. The prepared membranes were used in PV experiments performed on 94 wt% of ethanol aqueous solutions at 70°C. Single gas permeance of He, CO_2, N_2 or SF_6 was measured at 200°C prior to performing the PV experiments. An attempt was made to identify correlations between the single gas permeation experimental data and PV separation performance. Such relationships would offer a simple and quick method for the prediction of PV performance. To the best of the authors' knowledge, this report is the first to examine the relationships between PV performance and gas permeance using porous silica membranes.

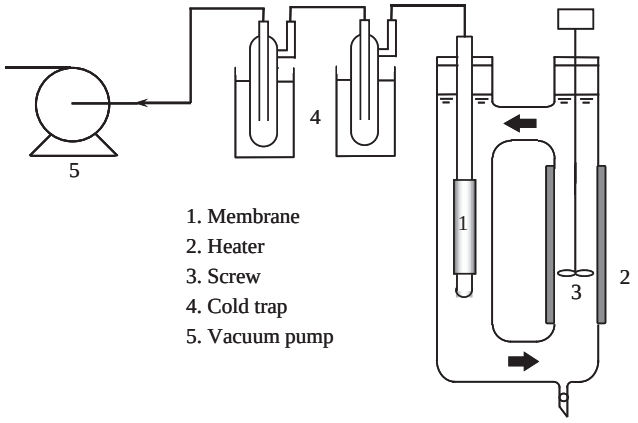

Fig. 1. Schematic figure of PV apparatus.

2. Experimental

2.1 Preparation of silica membranes

Porous α-alumina tubes (length: 10.0 cm, outer diameter: 1.0 cm, porosity: 50%) were used as supports that were coated with an α-alumina particle layer to create a smooth surface for additional coating. Pure silica or cobalt-doped silica sols were used as the top layer, and the membranes were fired at temperatures ranging from 350°C to 550°C. A total of 27 membranes were prepared in this study, including 10 pure silica membranes and 17 cobalt-doped silica membranes.

2.2 PV

PV experiments were carried out in a typical experimental apparatus equipped with a stirrer, heater and vacuum pump as shown in Fig. 1. All of the experiments were performed at 70°C using ethanol aqueous solutions consisting of 94 wt% ethanol. The solution was circulated at 1,600 rpm to reduce the effects of concentration and temperature polarization on water flux [3,5]. The permeated water was collected during a predetermined time interval using a cold trap that was cooled by liquid nitrogen. Silica membranes were dried at 180°C in an oven for at least 2 h before each experiment.

The separation factor was defined by the following equation:

$$\alpha = (Y_w/Y_e)/(X_w/X_e), \quad (1)$$

where Y_w and Y_e are the mole percentages of water and ethanol on the permeate side of the membrane,

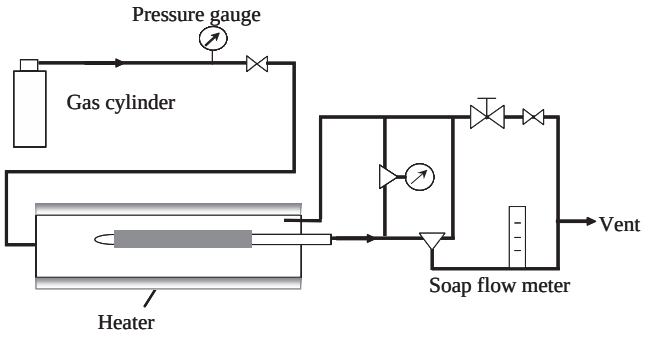

Fig. 2. Schematic flow chart of single gas permeation apparatus.

respectively. X_w and X_e are the mole percentages of water and ethanol on the feed side, respectively.

2.3. Single gas permeation

Before performing the PV experiments, single gas permeation was carried out in the apparatus as shown in Fig. 2. Permeance of He, CO_2, N_2 or SF_6 was measured at 200°C using a soap flow meter, and upstream pressure was controlled from 0.02 to 0.3 MPa, depending on the gas permeabilities. Downstream pressure was kept constant at atmospheric pressure. Before measurement, membranes were heated to 300°C under the flow of He to remove adsorbed water from inside the membrane pores.

3. Results and discussion

3.1. PV performance of silica membranes

Although porous silica membranes are stable in dry gases, they change their permeation characteristics in aqueous systems or in humid gaseous environments [7]. Thus, in the present study, it was necessary to confirm that the PV data used for prediction were collected after the membrane had already reached a steady state.

Fig. 3 shows a typical time course of PV performance of the membrane M16 measured at 70°C using a feed ethanol concentration of 94 wt%. Both water and ethanol flux decreased during the first several hundred minutes, and then reached a steady state after 600 min. After contact with water, the membrane underwent hydrolysis of siloxane bonds, followed by generation of silanol groups. Water and/or ethanol might have adsorbed tightly to the silanol groups. As a result, effective pore size was reduced, and permeation rate declined.

PV separation factor was plotted as a function of the total permeate flux for all membranes used in this study, as shown in Fig. 4. The circles and squares represent the

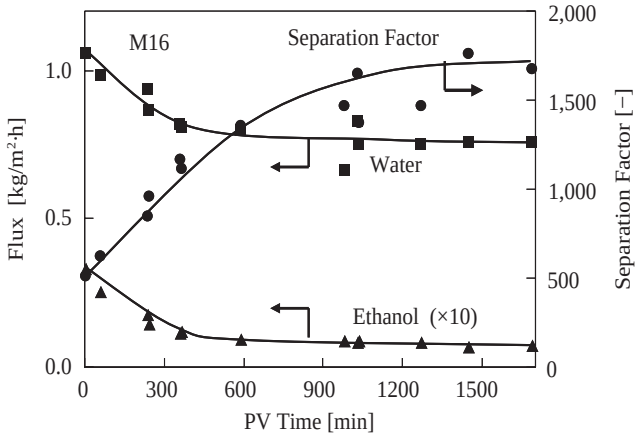

Fig. 3. Time course of PV performance of M16 at 70°C using a feed ethanol concentration of 94 wt%.

pure silica and cobalt-doped silica membranes, respectively. All data were collected after the membrane had reached a steady state. Total fluxes ranged from 0.1 to 2.2 kg/(m^2 h), while separation factors ranged from 3 to 5,700. Silica membranes with high separation factors showed relatively low flux and vice versa. All data points fell in the lower-left part, as illustrated by the trade-off curve in the figure. The exact values of PV flux and separation factor are shown in Table 1.

The reproducibility of PV performance was checked as follows. First, the PV experiment was carried out before gas permeance of He and N_2 was measured from 300°C to 50°C. Next, the PV experiment was carried out after the gas permeation experiments. Fig. 5 shows the PV fluxes and separation factor as a function of time using cobalt-doped silica membrane M24 for these two experiments. Solid symbols and lines

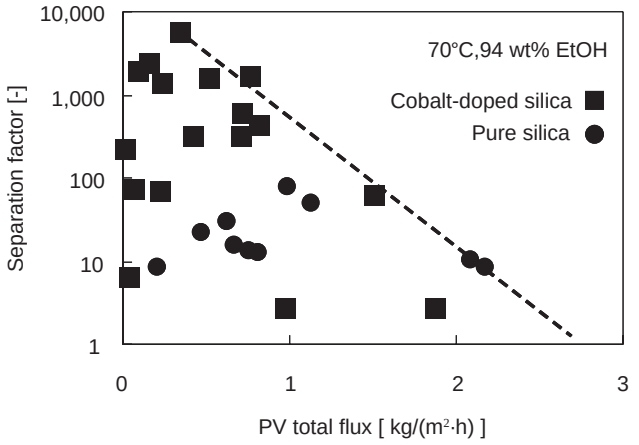

Fig. 4. PV separation factor as a function of total flux for all membranes used. Circles: pure silica membranes, squares: cobalt-doped silica membranes. Dotted line: trade-off curve.

Table. 1. PV data of all the membranes used in this study

	PV flux [kg/(m^2·h)]			Sep. factor
	Total	H_2O	EtOH	EtOH/H_2O
M01 p	1.137	0.841	0.296	48.5
M02 p	0.994	0.821	0.173	76.2
M03 p	2.083	0.77	1.313	10.5
M04 p	2.177	0.74	1.437	8.2
M05 p	0.213	0.074	0.139	8.2
M06 p	0.672	0.333	0.339	15.7
M07 p	0.818	0.374	0.444	12.7
M08	0.155	0.154	0.001	2380
M09	0.218	0.214	0.004	68.6
M10	0.068	0.056	0.012	72.1
M11	1.866	0.281	1.585	2.8
M12	0.968	0.146	0.822	2.8
M13	0.008	0.007	0.001	229
M14	0.031	0.009	0.022	6.4
M15	0.093	0.092	0.001	2030
M16	0.76	0.753	0.007	1670
M17	1.504	1.2	0.304	65
M18	0.818	0.788	0.03	436
M19	0.716	0.698	0.018	608
M20 p	0.758	0.344	0.414	13.1
M21 p	0.629	0.421	0.208	30.1
M22 p	0.471	0.278	0.193	21.8
M23	0.511	0.506	0.005	1630
M24	0.228	0.226	0.002	1400
M25	0.413	0.394	0.019	324
M26	0.7	0.668	0.032	321
M27	0.337	0.336	0.001	5720

Note: p after membrane number indicates a pure silica membrane, while unmarked are cobalt-doped membranes.

represent the first set of PV data, while open symbols and dashed lines show the PV data collected during the second experiment. The PV performances before and after gas permeation were consistent with one another, although water flux slightly decreased from 0.27 to 0.23 kg/(m^2 h), and ethanol flux only decreased from 0.0026 to 0.0025 kg/(m^2 h) after the gas permeation experiments. These changes might have been caused by densification of the membrane structure. Following the PV experiments, water and ethanol molecules would be adsorbed to the inside of the membrane pores. During single gas permeation experiments, the membrane was heated to 300°C for approximately 3 h. The OH groups reacted with O–Si–O groups in the membrane to form much denser silica networks. Water flux was reduced to a greater extent than ethanol. The separation factor showed no significant change, which means that the PV membrane performance during dehydration was unchanged. Thus, the reproducibility of PV performance was confirmed as adequate for prediction.

3.2. Single gas permeation

Membrane pore size and pore size distribution are very important for evaluation of performance. Nanopermporometry, which is based on Kelvin capillary condensation, can be used to determine pore size for pores larger than several nanometer in diameter [8]. However, for pores smaller than that, determination of exact pore size or of pore size distribution is difficult. Therefore, measurement of permeance for gases with different molecular diameters can be used to evaluate pore size of microporous membranes.

Fig. 6 shows single gas permeance of the cobalt-doped silica membrane M16. Permeance of He, CO_2, N_2 or SF_6 was plotted as a function of kinetic diameter. Judging from the Knudsen diffusion curve, which was calculated based on the permeance of N_2 and is shown in the figure by the dotted line, the separation mechanism is that of a molecular sieve. The permeance ratio of He/N_2 was approximately 21, while that of He/SF_6 was 118,500. The membrane consisted of relatively large pores compared with cobalt-doped membranes prepared in a steam atmosphere, which showed an H_2/N_2 ratio of approximately 730 [9]. A possible explanation for these results is the difference in top-layer firing conditions – air vs. steam. Firing in a steam atmosphere might have accelerated densification of the silica top layer. The high He/SF_6 ratio proved that the membrane had only a few pinholes larger than 0.55 nm, which is the kinetic diameter of SF_6.

The permeances of water and ethanol during PV using the same membrane are also plotted in Fig. 6. Both permeances seem to fall on the gas permeance kinetic-diameter-dependence curve. Water permeance was less than He and greater than CO_2, while ethanol permeance was less than N_2 and greater than SF_6. These results suggest that the transport mechanism of water and ethanol during PV is dominated by the molecular sieve, which is the same as the single gas transport mechanism. Therefore, it is reasonable to use gas permeance in the prediction of PV separation performance.

Operating temperature influences both the permeability coefficient of a membrane and the driving force for permeate flux, J, during PV processes, as follows [10]:

$$J = J_0 \exp(-E_j/RT), \quad (2)$$

where E_j is the activation energy of permeation. The activation energy E_j that is characteristic of temperature dependence of membrane permeability, can be evaluated by plotting $\ln(J/\triangle p)$ vs. $1/T$. Fig. 7 shows the temperature dependence of He and N_2 permeance

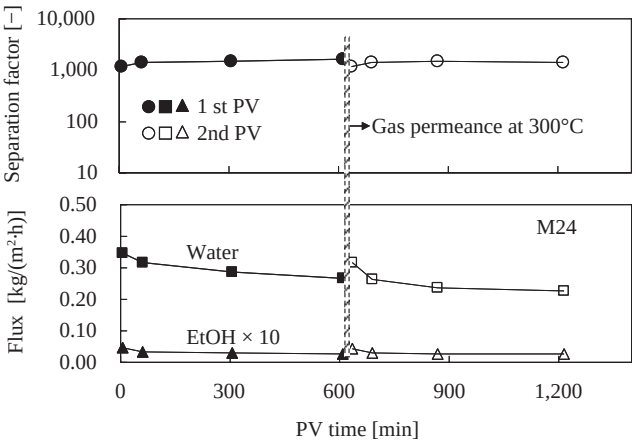

Fig. 5. PV performance change before and after single gas permeation measurement. Closed symbols with solid line: PV data collected prior to gas permeation. Open symbols with dashed line: PV performance after single gas permeation experiments.

measured before and after the PV experiments. The calculated activation energies of He and N_2 were approximately 2.6 and 2.3 kJ/mol, respectively. These values are relatively low compared with that of pure silica membranes. Kanezashi and Asaeda [11] studied the gas permeation characteristics of Ni-doped silica membranes (Si/Ni = 2/1). Using fresh membranes, the permeances of He and H_2 showed characteristics of slightly activated permeation, while N_2 permeance behaved in accordance with Knudsen's permeation mechanism, suggesting that N_2 permeated through a few pinholes left in the membrane. In the present study, the cobalt-doped silica membranes show activated permeation for both He and N_2, suggesting only a small number of pinholes existed in the membranes.

After the PV experiments, adsorbed molecules such as water and ethanol might have changed the membrane structure, so it was necessary to check the reproducibility of the single gas permeation data. Permeance of He and N_2 after PV dehydration of 94 wt% ethanol decreased only slightly compared with permeance data before the PV experiments. This result may be caused by slight shrinkage of membrane pores as a result of densification of the silica network. The reproducibility of single gas permeation before and after PV experiments was confirmed.

The effect of pretreatment temperature on single gas permeance was also investigated using a silica membrane. When membranes are kept in air, water vapor in the air can adsorb inside membrane pores and might affect single gas permeation performance with no pretreatment. To examine this effect, various pretreatment conditions were used before permeation

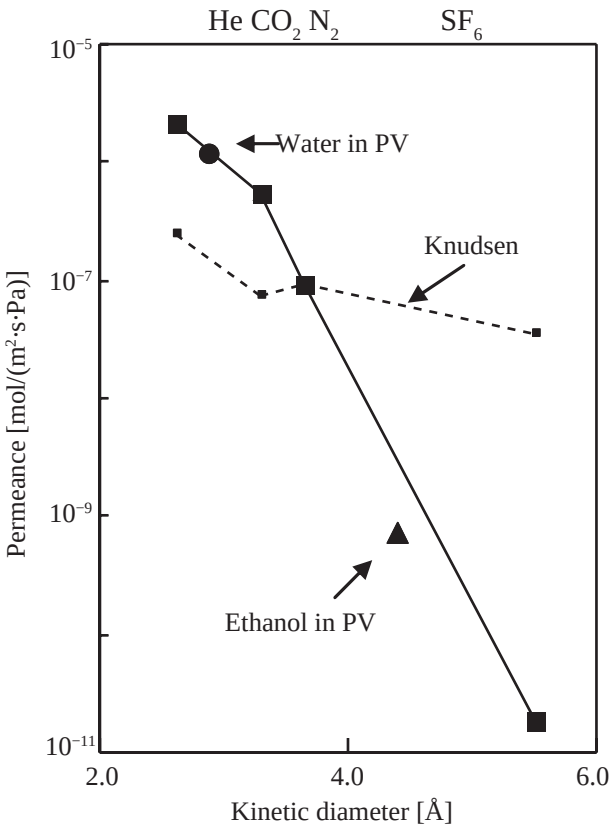

Fig. 6. Single gas permeance of Co-doped membrane as a function of kinetic diameter measured at 200°C plotted with PV ethanol and water permeance. The dashed line is the Knudsen diffusion curve calculated based on N_2 permeance.

measurement. In this experiment, the membrane was first kept in a dry oven at 20°C and 20 RH%, and then single gas permeance of He, N_2, SF_6 or CO_2 was

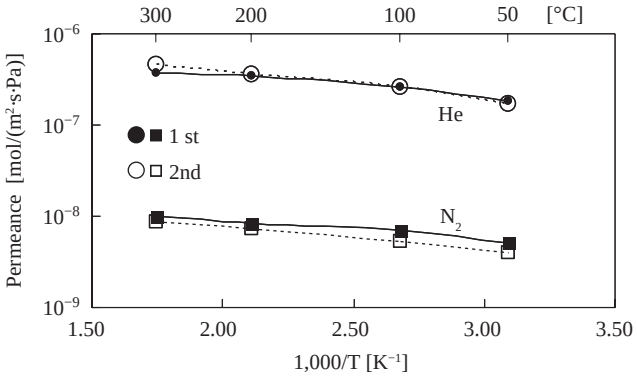

Fig. 7. Arrhenius plot of He and N_2 permeance measured before and after PV dehydration of ethanol and water at 70°C using 94 wt% ethanol. Closed symbols with solid line: data before PV, Open symbols with dashed line: data after PV experiments.

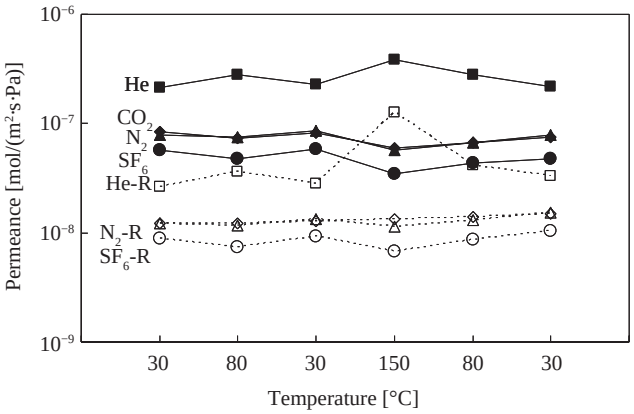

Fig. 8. Effect of pretreatment temperature on single gas permeance of silica membrane. Open symbol with dashed line: data after PV experiments.

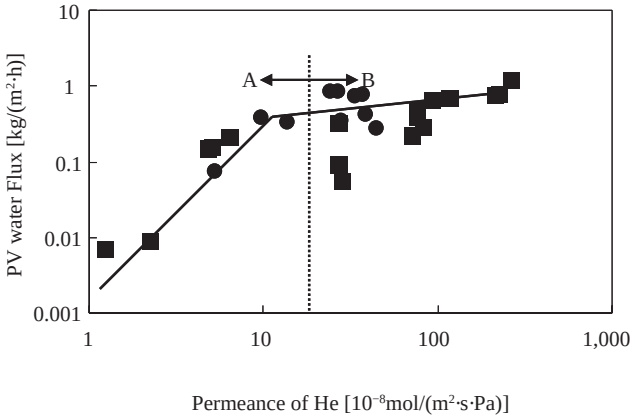

Fig. 9. Correlation between PV water flux and He permeance. Circles: pure silica membranes, squares: cobalt-doped silica membranes.

measured at 30°C. Next, the temperature was changed sequentially as follows: 80°C, 30°C, 150°C, 80°C and 30°C. Fig. 8 shows the gas permeance as a function of temperature. When the temperature was increased from 30°C, 80°C to 150°C, He permeance increased, while permeance of N_2, SF_6 and CO_2 decreased. This result indicates that activated diffusion through the membrane occurred. The permeance of the final measurement at 30°C increased only slightly compared with the first data point at 30°C. This observation suggests that heating to 150°C did not significantly affect membrane structure. The dotted lines show gas permeance of the same membrane measured after PV experiments. As explained previously, permeance decreased after PV. Permeances of He, CO_2, N_2, and SF_6 at 30°C increased after pretreatment of the membrane at 80°C and 150°C, suggesting that water adsorbed during PV was not completely removed at 80°C and affected gas permeation. Therefore, the optimal pretreatment temperature was determined to be 150°C or higher.

3.4. Correlation between PV and single gas permeation

As explained in the previous section (Fig. 6), the transport mechanism of water and ethanol during PV is mostly that of a molecular sieve, which is the same as that of single gas permeation. Reportedly, the molecular size of water is 0.296 nm, while that of ethanol is 0.430 nm [12]. The kinetic diameters of the gases used in the present study are as follows: He (0.26 nm), N_2 (0.364 nm) and SF_6 (0.55 nm). Therefore, it is reasonable to use gas permeance as a predictor of PV flux.

The kinetic diameter of He is slightly smaller than the molecular size of water, so water molecules are assumed to permeate through the same pores as He [13]. PV water flux was plotted against He permeance as shown in Fig. 9. PV water flux increased approximately linearly with He permeance when He permeance was less than 10^{-7} mol/ (m^2 s Pa) in area A. On the other hand, PV water flux increased only slightly with He permeance in the range of He permeance from 30 to approximately 600 $\times$ 10^{-8} mol/ (m^2 s kPa) in area B. This result can be attributed to the difference in transport mechanisms between pores of different diameters. In area A where He permeance is low, the membranes may consist of dense silica networks, water molecules possibly permeate through such small pores as do gaseous molecules. Therefore, the transport of water is identical to that of He, such that water flux increases almost linearly with He permeance. In area B, the mechanism of water transport may switch to liquid-phase permeation because of the larger pore diameter, as proposed by Yang et al. [13]. Capillary suction pressure, which is the major driving force for liquid water permeation through silica membranes, decreased. Thus, water flux increased only slightly even when the increase in He permeance was large. Another possible reason is the difference in resistance of the separation layer. In area A, most resistance can be attributed to the top layer because of the smaller pore size. Therefore, the driving forces for He and water exhibit a linear relationship. On the other hand, in area B, the supports also resist water transport during PV because of the evacuated condition. The support layer resistance has little effect on He permeation during viscous flow. It can be concluded that water flux during PV correlates with He permeance.

The permeance of SF_6, which has a molecular size of 0.55 nm, is considered to be an indicator of the number of pinholes in the membranes. During PV dehydration

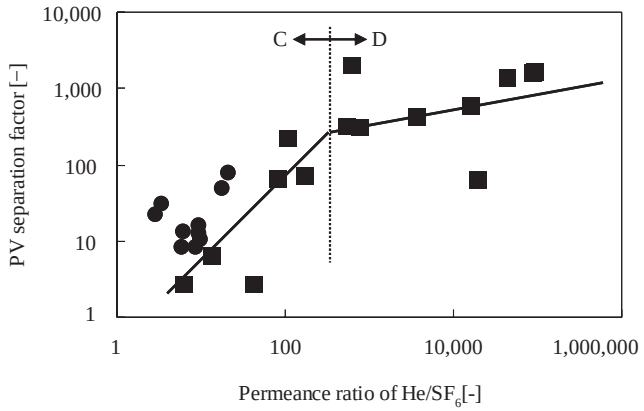

Fig. 10. Correlation between PV separation factor and permeance ratio of He/SF_6.

of ethanol/water solutions, fewer pinholes means lower ethanol permeate flux. As explained above, He permeance correlates well with water flux. So the single gas permeance ratio of He/SF_6 should be related to the PV separation factor. PV separation factor was plotted against the gas permeance ratio of He/SF_6 as shown in Fig. 10. The separation factor increased with the gas permeance ratio of He/SF_6 in area C, and increased only gradually even when the permeance increased markedly in area D.

In area C, the increased permeance ratio of He/SF_6 can be explained by a decrease in pore size or an increase in the sharpness of the pore size distribution curve, either of which will result in an increased separation factor. In other words, an increase in the permeance ratio of He/SF_6 can be achieved with smaller pores and fewer pinholes. In area D where permeance ratios of He/SF_6 were greater than 10,000, the silica membranes possibly had an increased number of pores that were slightly lager than He and smaller than water. As a result, even if the permeance ratio of He/SF_6 increased, which would shift the pore size distribution curve towards smaller pores, the separation factor increased only slightly. In conclusion, the PV separation factor was well correlated with the single gas permeance ratio of He/SF_6.

4. Conclusions

In this study, PV dehydration performance using a 94 wt% ethanol solution at 70°C was predicted using single gas permeation data for He, N_2, SF_6 and CO_2. During PV dehydration of the ethanol solution, both water and ethanol fluxes decreased during the first several hours and then reached a steady state. The separation factor increased and then reached a stable value. The reproducibility of PV performance and single gas permeation was checked and confirmed by changing the order in which the single gas and PV experiments were performed. Both He and N_2 permeance decreased with increasing temperature, which means the transport mechanism was mainly activated diffusion. He permeance was reasonably well correlated with PV water flux. The single gas permeance ratio of He/SF_6 was correlated with the PV separation factor.

References

[1] C. Casado, A. Urtiaga, D. Gorr and I. Ortiz, Pervaporative dehydration of organic mixtures using a commercial silica membrane: Determination of kinetic parameters, Sep. Pur. Technol., 42 (2005) 39–45.
[2] A. Lovasz, T. Farkas and P. Mizsey, Methodology for modelling of pervaporation: step from binary to ternary mixtures, Desalination, 241 (2009) 188–196.
[3] Y. Ma, J. Wang and T. Tsuru, Pervaporation of water/ethanol mixtures through microporous silica membranes, Sep. Pur. Technol., 66 (2009) 479–485.
[4] B. Bettens, S. Dekeyzer, B.V. der Bruggen, J. Degrève and C. Vandecasteele, Transport of pure components in pervaporation through amicroporous silica membrane, J. Phys. Chem. B, 109 (2005) 5216–5222.
[5] J. Yang and M. Asaeda, Permeation mechanism of water through microporous SiO_2-ZrO_2 membranes for separation of aqueous solutions of organic solvents by pervaporation, Sep. Pur. Technol., 32 (2003) 29–36.
[6] A.W. Thornton, T. Hilder, A.J. Hill and J.M. Hill, Predicting gas diffusion regime within pores of different size, shape and composition, J. Membr. Sci., 336 (2009) 101–108.
[7] B.-K. Sea, E. Soewito, M. Watanabe, K. Kusakabe, S. Morooka and S.S. Kim, Hydrogen recovery from a H2–H2O–HBr mixture utilizing silica-basedmembranes at elevated temperatures. 1. Preparation of H2O- and H2-selective membranes, Ind. Eng. Chem. Res., 37 (1998) 2502–2508.
[8] T. Tsuru, T. Hino, T. Yoshioka and M. Asaeda, Permporometry characterization of microporous ceramic membranes, J. Membr. Sci., 186 (2001) 257–265.
[9] R. Igi, T. Yoshioka, Y. H. Ikuhara, Y. Iwamoto and T. Tsuru, Characterization of Co-doped silica for improved hydrothermal stability and application to hydrogen separation membranes at high temperatures, J. Am. Ceram. Soc., 91 (2008) 2975–2981.
[10] X. Feng and R.Y.M. Huang, Estimation of activation energy for permeation in pervaporation processes, J. Membr. Sci., 118 (1996) 127–131.
[11] M. Kanezashi and M. Asaeda, Hydrogen permeation characteristics and stability of Ni-doped silica membranes in steam at high temperature, J. Membr. Sci., 271 (2006) 86–93.
[12] M.E. van Leeuwen, Derivation of Stockmayer potential parameters for polar fluids, Fluid Phase Equilibr., 99 (1994) 1–18.
[13] J. Yang, T. Yoshioka, T. Tsuru and M. Asaeda, Pervaporation characteristics of aqueous–organic solutions with microporous SiO_2–ZrO_2 membranes: Experimental study on separation mechanism, J. Membr. Sci., 284 (2006) 205–213.